Cross-conjugation controls the stabilities and photophysical properties of heteroazoarene photoswitches

Title: Cross-conjugation controls the stabilities and photophysical properties of heteroazoarene photoswitches

Authors: Daniel M. Adrion and Steven A. Lopez*

Affiliation: Department of Chemistry and Chemical Biology, Northeastern University, Boston, Massachusetts, 02115, United States

**Corresponding author:** s.lopez@northeastern.edu

Abstract

Azoarene photoswitches are versatile molecules that interconvert from their *E*-isomer to their *Z*-isomer with light. Azobenzene is a prototypical photoswitch but its derivatives can be poorly suited for *in vivo* applications such as photopharmacology due to undesired photochemical reactions promoted by ultraviolet light and its relatively short half-life ($t_{1/2}$) of the *Z*-isomer (2 days). Experimental and computational studies suggest that these properties (λ^{max} of the *E* isomer and $t_{1/2}$ of the *Z*-isomer) are inversely related. We identified isomeric azobisthiophenes and azobisfurans from a high-throughput screening study of 1700 azoarenes as photoswitch candidates with improved λ^{max} and $t_{1/2}$ values relative to azobenzene. We used density functional theory to predict the activation free energies, reaction free energies, and vertical excitation energies of the *E*- and *Z*-isomers of 2,2- and 3,3-substituted azobisthiophenes and azobisfurans. The half-lives depend on whether the heterocycles are π-conjugated or cross-conjugated with the diazo π-bond. The 2,2-substituted azoarenes both have $t_{1/2}$ values on the scale of 1 hour, while the 3,3-analogues have computed half-lives of 40 and 230 years (thiophene and furan, respectively). The 2,2-substituted heteroazoarenes have significantly higher λ^{max} absorptions than their 3,3-substituted analogues: 76 nm for azofuran and 77 nm for azothiophene.

Introduction

Photoswitches are molecules that are reversibly and chemically interconverted between two states with light. Azobenzene is the most widely studied photoswitch and has a well-documented synthesis via diazonium coupling reactions Azobenzene is the most widely studied photoswitch and has been synthesized using cross-coupling reactions[1-3], nucleophilic aromatic substitution[4], Bayer-Mills reactions[5-6], and diazonium coupling.[7] The relatively small size of azobenzene, along with the significant chemical and structural changes resulting from isomerization, has enabled its use for the spatiotemporal control of proteins, lipids, neurotransmitters, neurons, and carbohydrates.[8-20] Phenyl functionalization can improve photophysical properties for applications in chemical biology[21-22] and materials science.[23-27] Scheme 1 shows the photochemical *E* → *Z* conversion of azobenzene and the subsequent *Z* → *E* reversion, which can occur thermally or photochemically. Azobenzene requires ultraviolet light (320 nm) to promote the *E* → *Z* isomerization, limiting its utility in vivo due to undesired light-promoted dimerizations, destruction of living tissue from UV-light, and low light penetrability in living tissue.[17, 28-29] Further, the meta-stable *Z*-isomer thermally reverts to the *E* isomer and has a half-life ($t_{1/2}$) of 2

days at room temperature in acetonitrile. This relatively short half-life results in an unstable photostationary state (PSS), thus limiting photoswitch efficacy where bistability is needed.[14] As such, an ideal photoswitch features a long-lived $t_{1/2}$ (e.g., weeks to months), an E-isomer λ^{max} in the visible range, and well-separated λ^{max} values for the E and Z isomers to prevent bimodal isomerization.

Scheme 1. The azobenzene photoswitch reaction. The $E \rightarrow Z$ isomerization (top) occurs photochemically under UV light. The $Z \rightarrow E$ reversion (bottom) occurs thermally or photochemically under visible light.

E 320 nm / 440 nm or Δ Z
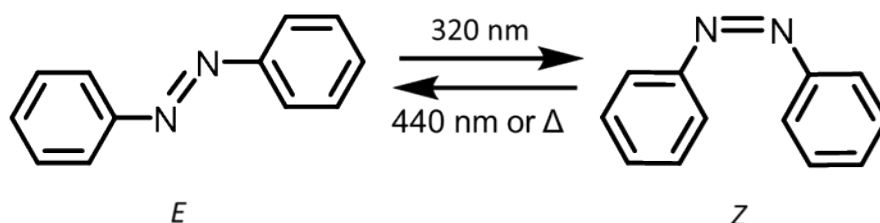
Woolley has shown how to tune the properties of azobenzenes through functionalizing the phenyl rings.[17] They have shown how the λ^{max} can be redshifted such that the azoarene will undergo photoswitching under visible light and in physiological conditions.[24, 30-31] Since the early 2000's, there has been an effort to design an ideal azoarene photoswitch substituted with aryl groups other than phenyl rings. Reports have shown that λ^{max} absorptions can be redshifted into the visible range by replacing phenyl groups with heteroaryl rings (benzodioxanes[32], diazinines[31], pyrroles[33], pyrazoles[34-35] and imidazoles[36-39]) and by functionalizing the aryl groups.[32, 40-54] These heteroazoarenes have relatively high $E \rightarrow Z$ photochemical reaction yields, ranging between 46-98%, and Z-isomer half-lives ranging from 1 second up to 46 years. The range in E-isomer λ^{max} for these heteroazoarenes is 310-720 nm, pushing them deep into the visible light range. There is an inverse relationship between λ^{max} and $t_{1/2}$ for these heteroazoarenes, those with the highest $t_{1/2}$ have the smallest λ^{max}. Scheme 2 shows heteroazoarenes with heteroaryl rings, and the heteroazoarenes of each type with the longest $t_{1/2}$ values are shown in Figure 1. Thermal $Z \rightarrow E$ reactions can proceed through inversion or rotation mechanistic pathways.[55-58] Past computational studies have found that the inversion mechanism is preferred for azoarene thermal $Z \rightarrow E$ isomerization reactions.[46, 56-61]

Scheme 2. (a) Nitrogen-containing azoarene photoswitches studied by Fuchter. (b) *Hemi*-azothiophene photoswitches studied by Wegner and Heindl. (c) Azobispyrazole photoswitches synthesized and studied by Li.
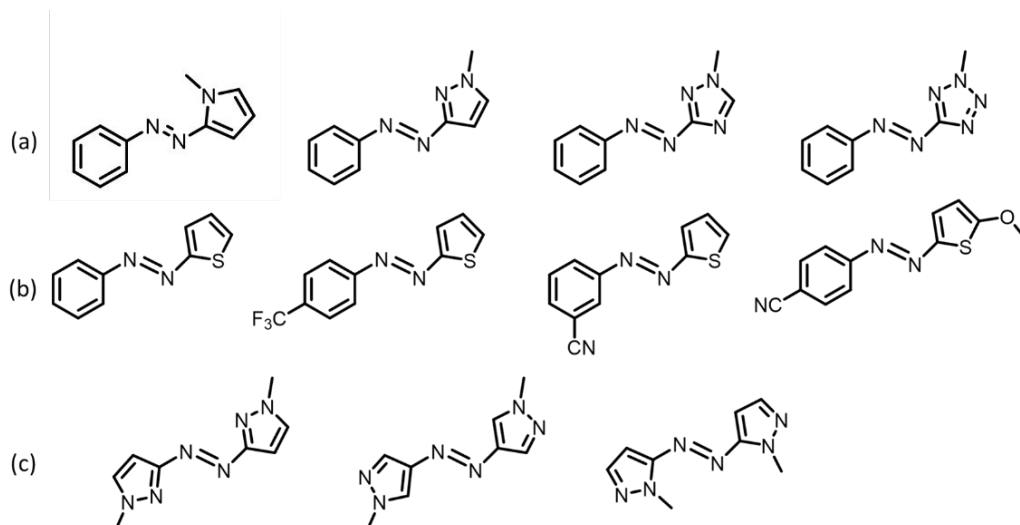
Thiophene-containing heteroazoarenes have well-separated E and Z absorption bands and a high yield of Z-isomer for the $E \rightarrow Z$ photoisomerization reaction (94-98%). 2-*hemi*-azothiophene and its derivatives have been studied by Wegner, Dreuw, and Wachtveitl[44-45] (Scheme 2b), and two (3,3) *bis*-azothiophenes (Figure 1) have been studied by Perry.[62] The unsubstituted 2-*hemi*-azothiophene (Scheme 2b, left) has a Z-isomer $t_{1/2}$ of 7 hours in acetonitrile. Wegner and Heindl[44] showed that electron-donating groups (EDG) at the phenyl *para* position (Me and OMe groups) of 2-*hemi*-azothiophenes lower the $t_{1/2}$ of the Z-isomer to 0.5 and 1.9 hours (methyl and methoxy substituent, respectively). Electron withdrawing groups (EWGs) increase the $t_{1/2}$ to 14.3 and 17.8 hours (CF$_3$ and CN, respectively). Substitution of the thiophene ring with an electron-donating group (OMe) lowered the $t_{1/2}$ to 2.8 hours. Installing push-pull substituents (OMe and CN groups) on an azothiophene lowered the $t_{1/2}$ to 9 minutes. The λ^{max} is 365 nm for the unsubstituted *hemi*-azothiophene and 405 nm for the push-pull *hemi*-azothiophene. All *hemi*-thiophene E-isomer λ^{max} values are red-shifted towards the visible range, an improvement over azobenzene. Figure 1 shows the heteroazoarenes photoswitches of each type with the longest measured half-lives.
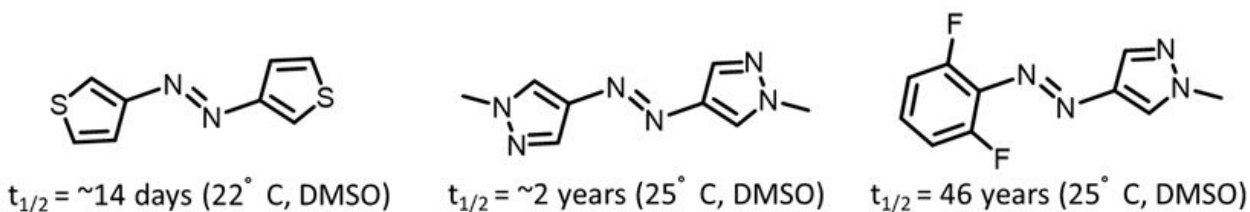

$t_{1/2}$ = ~14 days (22° C, DMSO) $t_{1/2}$ = ~2 years (25° C, DMSO) $t_{1/2}$ = 46 years (25° C, DMSO)

Figure 1. Three azoarene structures developed by Perry and co-workers (left), Li and co-workers (center), and Fuchter and co-workers (right). Experimental half-lives are provided, along with experimental conditions.

Although recent studies have increased the Z-isomer $t_{1/2}$ or the E isomer λ^{max}, experimental and theoretical studies on heteroazoarenes generally show an inverse relationship between $t_{1/2}$ and λ^{max}.[42, 63-65] The reason for this relationship has not been well defined; there is no clear

connection between how the *E*-isomer λ^{max} relates to the *Z*-isomer half-life. We have computed the thermal and photophysical properties of isomeric bis-heteroazoarenes photoswitches (two azobisfurans and two azobisthiophenes) using density functional theory (DFT) and time-dependent density functional theory (TD-DFT). The *Z* isomers of **1**, **2**, **3**, and **4** are shown in Figure 2. Watchtveitl and co-workers initially reported derivatives of **3-*Z***.[44-45] The (3,3)-azobisthiophene (**4**) and one derivative with ester groups substituted at the 2-position were synthesized, and UV/Vis spectra and *Z*-isomer half-lives were measured by Perry and co-workers.[62] These molecules had $t_{1/2}$ and λ^{max} values of 38 days and 316 nm (unsubstituted azothiophene) and 14 days and 350 nm (ester-substituted azothiophene).

The four heteroazoarenes presented in this study (**1**, **2**, **3**, and **4**) were obtained from the results of a high-throughput virtual screening (HVTS) study, which generated 1700 heteroazoarenes molecules for the VERDE materials database.[66] We calculated the λ^{max} and $t_{1/2}$ values for all molecules, which highlighted the 77 and 76 nm difference in λ^{max} between the (2,2) and (3,3) substituted structures and a 10^6 range in half-lives. We also highlight the cross-conjugated π-systems in **2** and **4**. Cross-conjugated molecules have incomplete π-delocalization, causing there to be two isolated π-systems in a molecule instead of one fully delocalized system. Cross-conjugation impacts photophysical properties by increasing the HOMO-LUMO gap, thus lowering λ^{max}. Schmidt and co-workers showed that cross-conjugated diynes have lower λ^{max} values than fully conjugated diynes by up to 39 nm because the frontier molecular orbitals are not fully delocalized.[67] Krenske and co-workers showed that thiol nucleophilic additions were accelerated when the enones were cross-conjugated.[68] Sherburn accessed dendralenes with cross-coupling chemistry and found enhanced reactivity towards dienophiles in Diels-Alder reactions. Cross-trienamines were used in asymmetric organocatalysis by Jorgensen and co-workers; experiments and computations demonstrate that relatively high-lying HOMOs increase the cycloaddition reactivity towards oxindoles and azlactones.[69-70] Cross-conjugated trienamines have been used to enantioselectively access polycyclic natural products such as Lycopladine[71], bisorbicillinoids[72], and sesquiterpenes.[73]
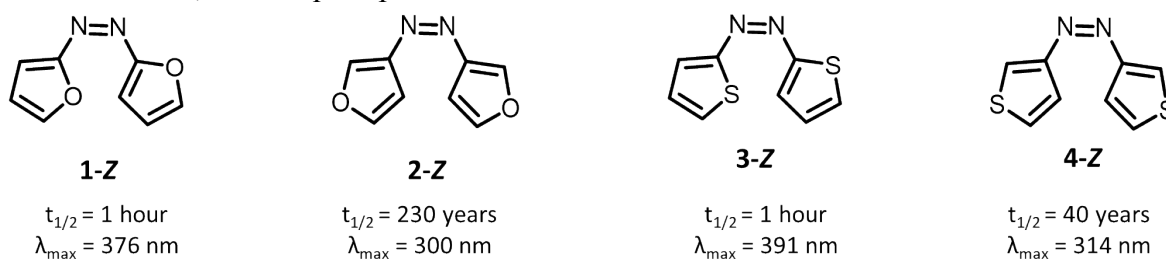

1-*Z*	**2-*Z***	**3-*Z***	**4-*Z***
$t_{1/2}$ = 1 hour	$t_{1/2}$ = 230 years	$t_{1/2}$ = 1 hour	$t_{1/2}$ = 40 years
λ_{max} = 376 nm	λ_{max} = 300 nm	λ_{max} = 391 nm	λ_{max} = 314 nm

Figure 2. Four heteroazoarenes considered for this study and their calculated $t_{1/2}$ and λ^{max} values.

Results and discussion

High-Throughput Screening Process. The initial screening of azoarenes was carried out using the high-throughput screening workflow highlighted in an earlier paper from our group.[66] An initial set of azoarenes used included an unsubstituted azobenzene molecule, along with azothiophene, azofuran, and azopyrrole. These molecules are presented in Scheme 3.
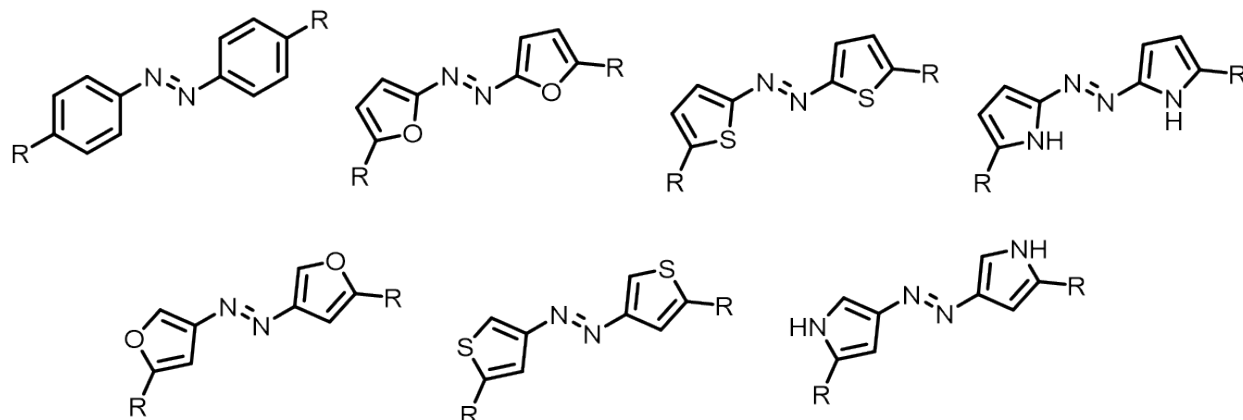
Scheme 3. Molecules used for the initial high-throughput screening.

Using the substitution patterns from the workflow, we generated 1,540 molecules for initial screening, and measured their λ^{max}. From this initial screening, we observed a large difference in the λ^{max} of positional isomers **1** and **2**, and **3** and **4**. Next, we calculated the thermal free energy barriers for the $Z \rightarrow E$ thermal isomerization reaction for the two sets of positional isomers. These results highlighted the differences in $t_{1/2}$ between the (2,2) (**1** and **3**) and (3,3) (**2** and **4**) azoarenes.

We performed IRC calculations and geometry optimizations to obtain the reactive conformers for the lowest energy transition states of azofurans **1-TS** and **2-TS**, and azothiophenes **3-TS** and **4-TS**. Figure 3 shows the optimized reactants **1-Z** and **2-Z**, along with their optimized transition structures **1-TS** and **2-TS**, and Figure 4 shows the energies and geometries of transition structures of **(3-4)-Z**, **(3-4)-TS**. **2-Z** has an isomerization barrier that is 8.5 kcal mol^{-1} higher than the corresponding azofuran **1-Z**. We sought to understand how the electronic structures of **(1-4)-Z** affect the 10^6-fold range in half-lives. The transition states feature coplanar aryl groups; we quantify this coplanarity with an out-of-plane angle (θ). θ is the angle between two normal vectors to the planes of the aryl rings. We will first discuss the structures of the azofuran reactants **1-Z** and **2-Z**, and inversion $Z \rightarrow E$ transition structures, **1-TS** and **2-TS**. We quantify the differences in geometry between the reactants and transition states by measuring the ring co-planarity (θ) and key bond lengths that describe the changes in π-conjugation. We then compare these structures to **3** and **4** to understand how bisazothiophenes differ from bisazofurans. The frontier molecular orbitals were computed; we demonstrate how their energies and overlap are affected by cross-conjugation.
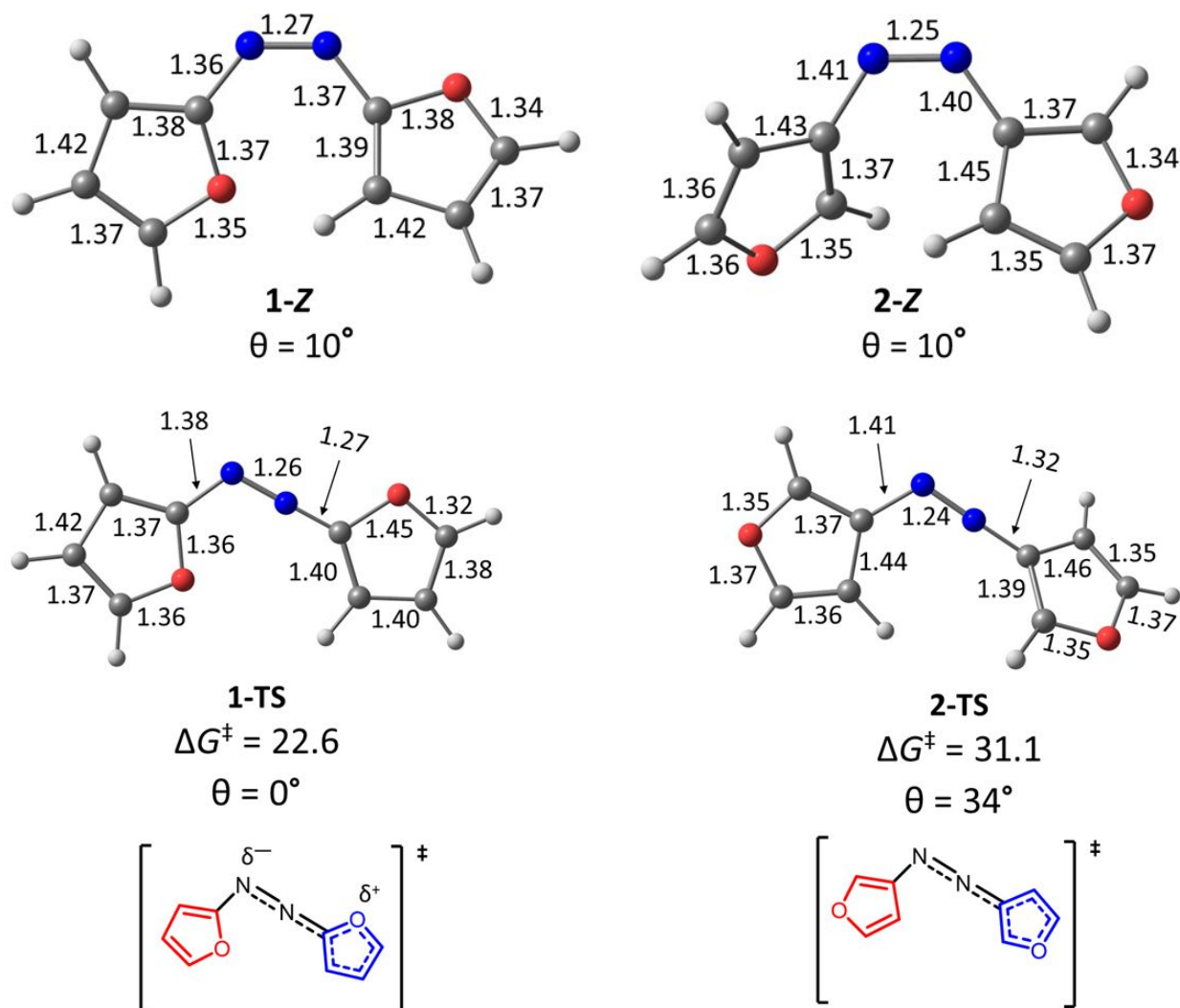
4

Figure 3. Top: Optimized azofuran reactive conformers **1-Z** (left) and **2-Z** (right). Bond lengths are given in Angstroms (Å). The dihedral angle (θ) measures the CNNC angle. Bottom: Computed azofuran transition states **1-TS** (left) and **2-TS** (right). Bond lengths are shown in angstroms (Å). The out-of-plane angle, θ, measures the relative planarity of the furan rings.

The top portion of Figure 3 shows the optimized reactant geometries **1-Z** and **2-Z**. The C–C bond lengths in the furan rings are 1.37-1.42 Å for **1-Z** and 1.35-1.45 Å for **2-Z**. These distances correspond to aromatic C–C bond lengths. The C–O bonds range from 1.34-1.38 Å for **1-Z** and 1.34-1.37 Å for **2-Z**, all consistent with aromatic C–O bond lengths in furan rings. The two reactants also have the same CNNC dihedral angle (θ=10°), indicating equivalent relative planarities of the aryl rings in both structures. The N=N π-bonds are 1.27 Å in **1-Z** and 1.25 Å in **2-Z**. The C–N bonds in **2-Z** (1.40 and 1.41 Å) are significantly longer than those in **1-Z** (1.36 and 1.37 Å). The C–N bond lengths in **1-Z** are consistent with aromatic C–N bond distances, while the C–N bond distances in **2-Z** more closely resemble C–N single bonds. The shorter C–N bonds

5

and the longer N=N bond indicate more electron delocalization between the furan rings in **1-Z** than **2-Z**. We will now turn our attention to the transition structures **1-TS** and **2-TS**.

The $\Delta G^{\ddagger}$ for **1-TS** is 22.6 kcal mol^{-1}, and the $\Delta G^{\ddagger}$ for **2-TS** is 31.1 kcal mol^{-1} for the thermal $Z \rightarrow E$ isomerization. The difference in activation free energies ($\Delta\Delta G^{\ddagger}$) is 8.5 kcal mol^{-1}, corresponding to half-lives of one hour and 230 years, respectively. **1-TS** and **2-TS** involve a rehybridization of one of the N atoms, which corresponds to a linearization of the NNC2 and NNC3 angles (NNC angles of 179° and 178°, respectively). The N=N diazo bond lengths for **1-TS** and **2-TS** are 1.27 Å and 1.25 Å, respectively. These bond lengths are shorter than in the Z-isomers, where they are 1.28 and 1.26 Å for **1-Z** and **2-Z**, respectively.

The C–C bond lengths in the furan rings range from 1.35 to 1.46 Å, consistent with aromatic C–C bond lengths in the crystal structure of furan (1.32 to 1.43 Å). The C–O bonds have a small range in **1-Z** (1.34-1.38 Å) but have a larger range in **1-TS** (1.32-1.45 Å). The 1.32 Å C–O bond length is consistent with an aromatic C–O bond length, while 1.45 Å corresponds to a C–O single bond. The furan on the left side (red) of **1-TS** has identical C–O bond lengths (1.36 Å), while the furan on the right side (blue) of **1-TS** has C–O bond lengths of 1.32 and 1.45 Å. This disparity is caused by an asymmetric resonance-donation of a furan lone pair orbital in **1-TS** relative to **1-Z**. The C–N bond lengths flanking the diazo bond are 1.38 Å and 1.26 Å. The C–N bond connecting the blue furan to the N=N bond significantly shortens in **1-TS** from **1-Z** (1.26 Å from 1.37 Å), indicating increased π-character, while the other C–N bond is nearly unchanged from **1-TS** to **1-Z** (1.38 Å and 1.36 Å, respectively). The relative planarity between the two rings (θ) is significantly different for **1-TS** and **2-TS**. The two furan rings in **1-TS** are fully coplanar (θ=0°), maximizing the π-conjugation between them. **2-TS** is a cross-conjugated azofuran, which implies that π-conjugation is between part of the aromatic π-system of the blue furan with the diazo bond throughout the reaction. While **2-TS** also involves a rehybridization of one of the N-atoms, the furans are not coplanar (θ=34°) because the rings are not electronically communicating through the diazo bond. The difference in the C–O bond lengths in **2-TS** is 0.03 Å (1.35 and 1.38 Å), which suggests that the delocalization of oxygen lone pairs substantially decreases. The C–N bonds flanking the N=N bond are 1.42 and 1.32 Å. As such, azoarenes featuring cross-conjugation do not have full π-delocalization across the diazo bond. This phenomenon results in the 8.5 kcal mol^{-1} $\Delta\Delta G^{\ddagger}$ of these isomeric azofurans. The (2,2)-diazofurans are 10^6-fold more reactive than the (3,3)-diazofurans. We now turn our attention to the azothiophenes **3** and **4**.
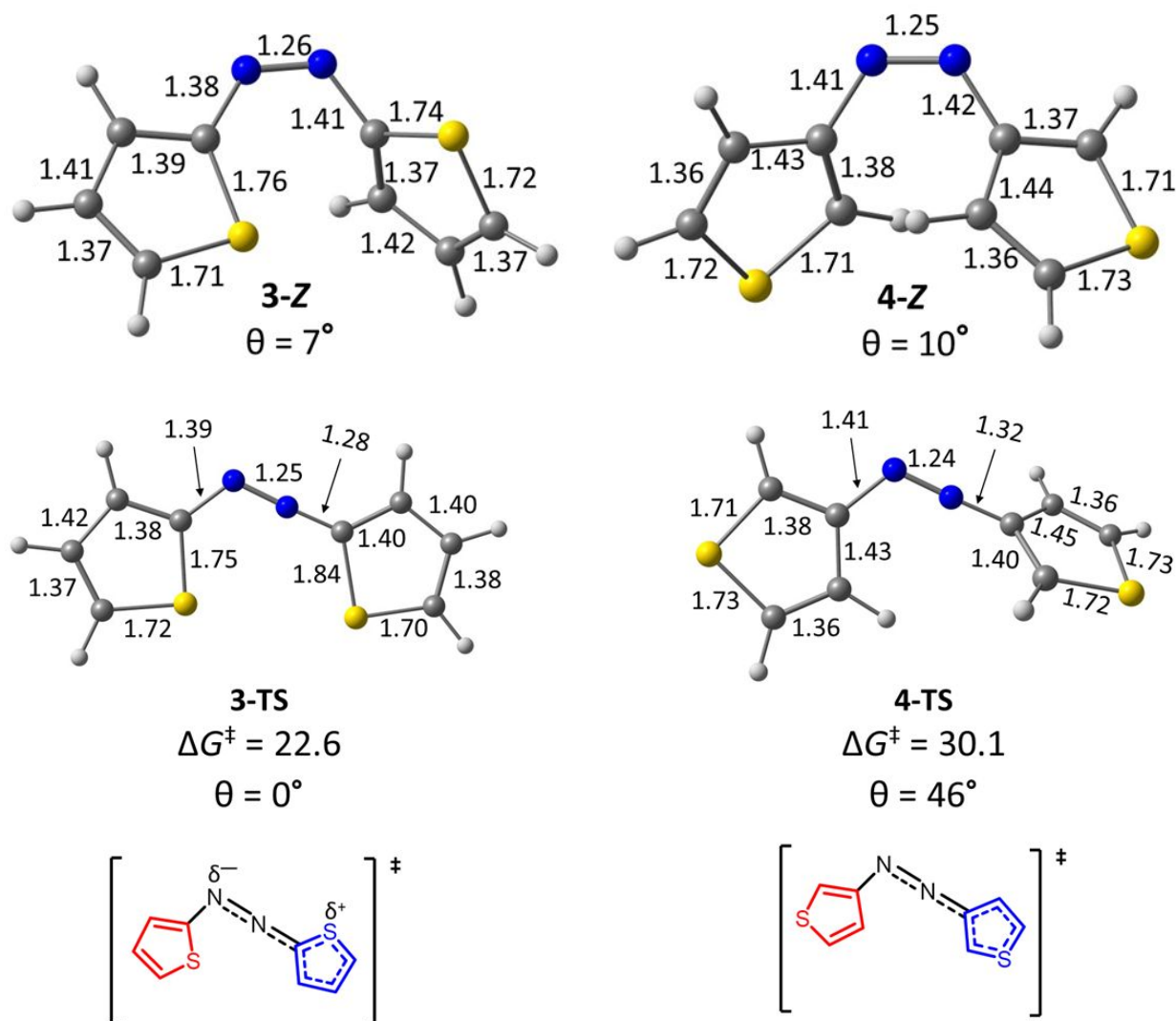
Figure 4. Top: Optimized azothiophene reactive conformers **3-Z** (left) and **4-Z** (right). The bond lengths are given in Angstroms (Å). The dihedral angle (*θ*) measures the CNNC angle. Bottom: Computed azothiophene transition states **3-TS** (left) and **4-TS** (right). Bond lengths are shown in angstroms (Å). The out-of-plane angle, *θ,* measures the relative planarity of the thiophene rings.

The C–C bond lengths in the thiophene rings range from 1.37 to 1.42 Å for **3-Z** and 1.36 to 1.44 Å for **4-Z**. These distances correspond to aromatic C–C bond lengths. (1.35 to 1.44 Å in the crystal structure of thiophene). The C–S bond lengths range from 1.71-1.76 Å for **3-Z** and 1.71-1.73 Å for **4-Z**. **3-Z** has a CNNC dihedral of 7°; **4-Z** has a CNNC dihedral of 10°. The structural differences between the two reactants are present in the bond distances of the CNNC bonds. The N=N bonds are 1.26 Å in **3-Z** and 1.25 Å in **4-Z**. The C–N bonds in **4-Z** (1.41 and 1.42 Å) are longer than the analogous bonds in **3-Z** (1.38 and 1.41 Å). The shorter C–N bond length in **3-Z** is consistent with an aromatic C–N bond, and the longer C–N bond lengths in **4-Z** are consistent with single bonds. The shorter C–N bonds and the longer N=N bond indicate that **3-Z** has more electron delocalization between the two thiophene rings than **4-Z**.

7

The $\Delta G^{\ddagger}$ for **3-TS** is 22.6 kcal mol^{-1}, and the $\Delta G^{\ddagger}$ for **4-TS** is 30.1 kcal mol^{-1}. The difference in activation free energies ($\Delta\Delta G^{\ddagger}$) is 7.5 kcal mol^{-1}, corresponding to half-lives of one hour and 40 years, respectively. Transition structures **3-TS** and **4-TS** involve rehybridization about one of the N atoms and have nearly linear NNC$_2$ and NNC$_3$ angles (179° and 178°, respectively). The N=N bonds are shorter in **3-TS** (1.25 Å) and **4-TS** (1.24 Å) relative to their corresponding reactants (1.26 Å and 1.25 Å, respectively). These bond lengths shorten as the azothiophenes reach their respective transition structure geometries, resulting from the rehybridization of one of the N atoms.

The C–C bond lengths in the thiophene rings range from 1.36 to 1.45 Å, which is consistent with aromatic C–C bond lengths in thiophene rings. The C–S bonds are 1.71-1.76 Å in **3-Z** but diverge in **3-TS** (1.70-1.84 Å) because one of the sulfur lone pairs is delocalized through the transition structure. This phenomenon results in the zwitterionic electronic structure shown in Figure 7. The shorter bond length resembles a C–S double bond,[74] while the longer bond corresponds to a broken C–S π-bond (the aromatic C–S bonds in the crystal structure of thiophene are 1.74 Å).[74] The red thiophene ring has two nearly identical C–S bond lengths (with lengths of 1.72 and 1.75 Å), indicating aromatic C–S bond lengths. The C–N bonds flanking the diazo bond differ substantially (1.39 and 1.28 Å) in **3-TS**. The C–N bond connecting the blue thiophene to the N=N bond significantly shortens in **3-TS** from **3-Z** (1.28 Å from 1.38 Å), indicating increased π-conjugation, while the other C–N bond is relatively unchanged from **3-Z** to **3-TS** (1.41 and 1.39 Å, respectively). The thiophene rings of **4-TS** deviate significantly from coplanarity (θ=46°) due to the decreased conjugation across the diazo bond. The difference in the C–S bond lengths in **4-TS** is 0.02 Å (1.71-1.73 Å), suggesting that the sulfur delocalization effect significantly decreased relative to **3-TS**. The C–N bonds flanking the N=N bond are 1.41 Å and 1.32 Å. These corresponding bond lengths in **3-TS** are shorter (1.39 Å and 1.28 Å) due to increased π-conjugation.

We performed time-dependent density functional theory (TD-DFT) calculations to predict the nature of the electronic transitions and vertical excitation energies of the *E*-isomers. The corresponding λ^{max} derived from the vertical excitation energies of **1-E**, **2-E**, **3-E**, and **4-E** are 382, 304, 400, and 317 nm, respectively. All electronic transitions shown below correspond to a single excitation from the HOMO to the LUMO ($\pi \rightarrow \pi^{*}$). The experimental λ^{max} of (3,3) azothiophene is 332 nm.[62] **1-E,** and **3-E** have λ^{max} which are redshifted by 78 nm and 83 nm relative to **2-E** and **4-E**, respectively. To understand the origin of the 96 nm range in λ^{max} along this series, we computed the frontier molecular orbitals (FMOs) for **1-E**, **2-E**, **3-E**, and **4-E** (Figure 5).
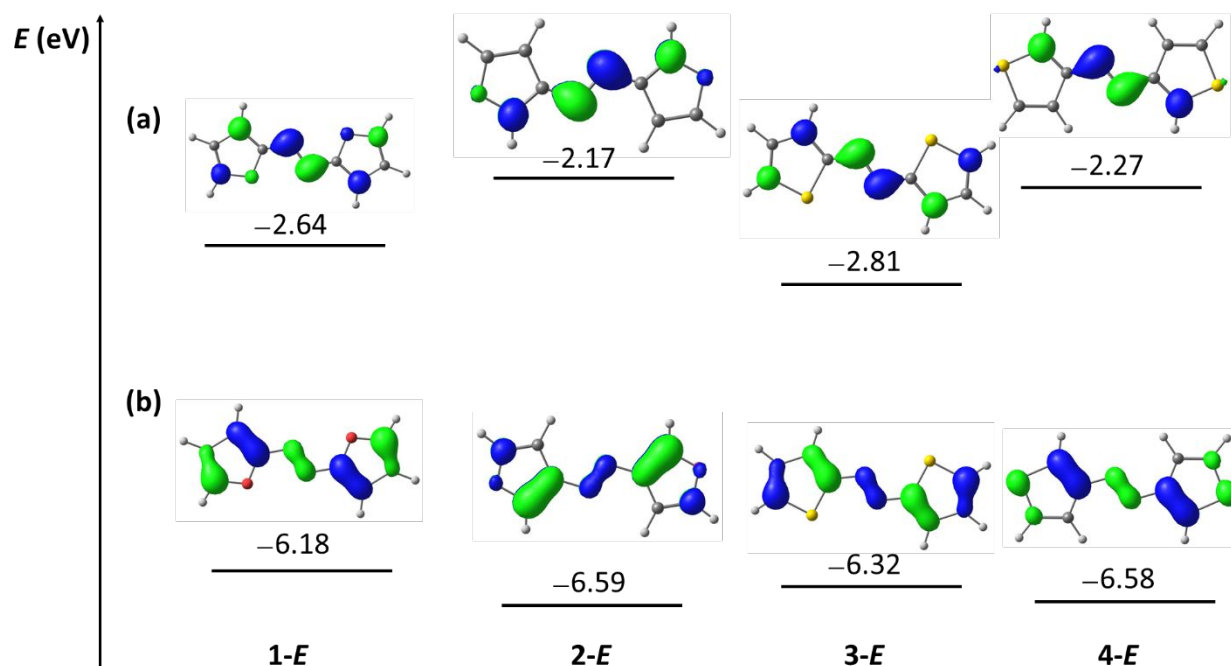
Figure 5. Computed LUMOs (a) and HOMOs (b) of **1-*E***, **2-*E***, **3-*E***, and **4-*E***. The orbitals were calculated with PBE0-D3(BJ)/6-31+G(d,p) and IEFPCM^{H2O}.

1-*E* and **3-*E*** have fully delocalized π-systems across the diazo bond, while **2-*E*** and **4-*E*** show interrupted π-electron density due to their cross-conjugated nature. The cross-conjugated π-systems in **2-*E*** and **4-*E*** affect the energies and energy gaps of the frontier molecular orbitals (HOMO and LUMO). The delocalization effect in **1-*E*** and **3-*E*** leads to higher-lying HOMOs and lower-lying LUMOs relative to **2-*E*** and **4-*E***, leading to increased HOMO-LUMO gaps. The HOMO for **1-*E*** is –6.18 eV, 0.41 eV higher than the HOMO for **2-*E*** (–6.59 eV), and the HOMO for **3-*E*** is –6.32 eV, 0.25 eV higher than the HOMO for **4-*E*** (–6.58 eV). The LUMO for **1-*E*** is –2.64 eV, which is 0.47 eV lower than the LUMO for **2-*E*** (–2.17 eV), and the LUMO for **3-*E*** is –2.81 eV, 0.53 eV lower than the LUMO for **4-*E*** (–2.27 eV). The HOMO-LUMO gaps of **1-*E*** and **2-*E*** are 3.54 eV and 4.42 eV (a 0.88 eV difference), and the same gaps are 3.51 eV and 4.31 eV for **3-*E*** and **4-*E***, a difference of 0.80 eV. These results suggest that the cross-conjugated π-systems lead to lower energy HOMO and higher energy LUMO orbitals for azoarene photoswitches, which is consistent with the effects that cross-conjugation has on other molecule systems. The large frontier molecular orbital gaps cause higher vertical excitation energies and smaller λ^{max}.

Conclusion

We have used DFT to determine the photophysical properties and thermal stabilities of four *bis*-diazoarene photoswitches. We predict that the thermal half-lives of the isomeric *Z*-isomers range from hours to years. The (3,3)-substituted isomers (**2** and **4**) have cross-conjugated π-systems, significantly affecting the photophysical and thermal properties. This truncated π-

conjugation leads to large optical gaps, thus requiring UV light for photoswitching (300 nm for **2-*E*** and 314 nm for **4-*E***). Those with fully π-conjugated systems (**1-*E*** and **3-*E***) contain relatively small optical gaps, which enable visible light photoswitching (376 nm and 391 nm, respectively). The extent of π-conjugation strongly influences the transition structures and thermal half-lives of the *Z*-isomers. **1-*Z*** and **3-*Z*** have a small $\Delta G^{\ddagger}$, which translates to a $t_{1/2}$ of one hour. **2-TS** and **4-TS** are higher in energy due to the limited π-delocalization, and the $t_{1/2}$ is in the range of 40-230 years. Towards photoswitches with long half-lives and visible-light absorption, we recommend functionalizing diazo functional groups with two aryl groups, one cross-conjugated and one fully conjugated. For example, an azoarene with a 3-thiophene ring and a para-nitrophenyl ring. The strongly withdrawing nature of the nitro group redshifts the λ^{max}, while the cross-conjugation contributes to higher activation free energies and long $t_{1/2}$. We are currently exploring non-symmetric azoarenes with one phenyl ring and one cross-conjugated aryl ring (thiophene or furan) flanking the diazo bond.

Computational methods

We performed DFT calculations to predict the activation free energies ($\Delta G^{\ddagger}$) of (**1–4-*Z***). We computed the structures and energies of the *Z*-isomer, *E*-isomer, and transition structure for each reaction. First, the transition structures were optimized using the *EZ*-TS code recently reported by our group.[75] After locating the lowest energy transition states, we ran intrinsic reaction coordinate (IRC) calculations and optimized the reactive conformers corresponding to the reactant (*Z*-isomer) and product (*E*-isomer) for each thermal $Z \rightarrow E$ isomerization. All calculations were performed using the Gaussian 16 software.[76] The PBE0-D3BJ[77]/6-31+G(d,p)[78] model chemistry was used for all geometry optimizations and frequency calculations. Vertical excitation energies were calculated using TD-DFT[79] with the ωB97X-D[80]/6-311+G(d,p) model chemistry in IEFPCM[water].[81] The first 10 singlet excited states were calculated for all TD-DFT calculations.

TOC image

References

1.   Wang, Y.; Xie, R.; Huang, L.; Tian, Y.-N.; Lv, S.; Kong, X.; Li, S., Divergent synthesis of unsymmetrical azobenzenes via Cu-catalyzed C–N coupling. *Organic Chemistry Frontiers* **2021,** *8* (21), 5962-5967.

2.   Kılınçarslan, R.; Erdem, E.; Kocaokutgen, H., Synthesis and spectral characterization of some new azo dyes and their metal complexes. *Transition Metal Chemistry* **2006,** *32* (1), 102-106.

3.   Staubitz, A.; Walther, M.; Kipke, W.; Schultzke, S.; Ghosh, S., Modification of Azobenzenes by Cross-Coupling Reactions. *Synthesis* **2021,** *53* (07), 1213-1228.

4.   Hartmann, H,; Schulze, M.; Guenther, R., Nucleophilic Substitution in Arylazo Phenols - a Simple Route for Preparing Chlorosubstituted Azobenzenes, *Dyes and Pigments,* **1991,** *15,* 255-262.

5.   Heindl, A. H.; Wegner, H. A., Starazo triple switches - synthesis of unsymmetrical 1,3,5-tris(arylazo)benzenes. *Beilstein J Org Chem* **2020,** *16*, 22-31.

6.   Slavov, C.; Yang, C.; Schweighauser, L.; Boumrifak, C.; Dreuw, A.; Wegner, H. A.; Wachtveitl, J., Connectivity matters - ultrafast isomerization dynamics of bisazobenzene photoswitches. *Phys Chem Chem Phys* **2016,** *18* (22), 14795-804.

7.   Merino, E., Synthesis of azobenzenes: the coloured pieces of molecular materials. *Chem Soc Rev* **2011,** *40* (7), 3835-53.

8.   Morstein, J.; Trauner, D., Photopharmacological control of lipid function. *Methods Enzymol* **2020,** *638*, 219-232.

9.   Doroudgar, M.; Morstein, J.; Becker-Baldus, J.; Trauner, D.; Glaubitz, C., How Photoswitchable Lipids Affect the Order and Dynamics of Lipid Bilayers and Embedded Proteins. *J Am Chem Soc* **2021**.

10.   Korbus, M.; Backe, S.; Meyer-Almes, F. J., The cis-state of an azobenzene photoswitch is stabilized through specific interactions with a protein surface. *J Mol Recognit* **2015,** *28* (3), 201-9.

11.   Albert, L.; Vazquez, O., Photoswitchable peptides for spatiotemporal control of biological functions. *Chem Commun (Camb)* **2019,** *55* (69), 10192-10213.

12.   Trads, J. B.; Hull, K.; Matsuura, B. S.; Laprell, L.; Fehrentz, T.; Gorldt, N.; Kozek, K. A.; Weaver, C. D.; Klocker, N.; Barber, D. M.; Trauner, D., Sign Inversion in Photopharmacology: Incorporation of Cyclic Azobenzenes in Photoswitchable Potassium Channel Blockers and Openers. *Angew Chem Int Ed Engl* **2019,** *58* (43), 15421-15428.

13.   Cheng, B.; Morstein, J.; Ladefoged, L. K.; Maesen, J. B.; Schiott, B.; Sinning, S.; Trauner, D., A Photoswitchable Inhibitor of the Human Serotonin Transporter. *ACS Chem Neurosci* **2020,** *11* (9), 1231-1237.

14.   Broichhagen, J.; Frank, J. A.; Trauner, D., A roadmap to success in photopharmacology. *Acc Chem Res* **2015,** *48* (7), 1947-60.

15.   Banghart, M.; Borges, K.; Isacoff, E.; Trauner, D.; Kramer, R. H., Light-activated ion channels for remote control of neuronal firing. *Nat Neurosci* **2004,** *7* (12), 1381-6.

16.   Hamon, F.; Djedaini-Pilard, F.; Barbot, F.; Len, C., Azobenzenes—synthesis and carbohydrate applications. *Tetrahedron* **2009,** *65* (49), 10105-10123.

17.   Beharry, A. A.; Woolley, G. A., Azobenzene photoswitches for biomolecules. *Chem Soc Rev* **2011,** *40* (8), 4422-37.

18.   Fehrentz, T.; Schonberger, M.; Trauner, D., Optochemical genetics. *Angew Chem Int Ed Engl* **2011,** *50* (51), 12156-82.

19.   Broichhagen, J.; Podewin, T.; Meyer-Berg, H.; von Ohlen, Y.; Johnston, N. R.; Jones, B. J.; Bloom, S. R.; Rutter, G. A.; Hoffmann-Roder, A.; Hodson, D. J.; Trauner, D., Optical Control of Insulin Secretion Using an Incretin Switch. *Angew Chem Int Ed Engl* **2015,** *54* (51), 15565-9.

20.   Laprell, L.; Repak, E.; Franckevicius, V.; Hartrampf, F.; Terhag, J.; Hollmann, M.; Sumser, M.; Rebola, N.; DiGregorio, D. A.; Trauner, D., Optical control of NMDA receptors with a diffusible photoswitch. *Nat Commun* **2015,** *6*, 8076.

21.   Hull, K.; Morstein, J.; Trauner, D., In Vivo Photopharmacology. *Chem Rev* **2018,** *118* (21), 10710-10747.

22.   Tochitsky, I.; Kienzler, M. A.; Isacoff, E.; Kramer, R. H., Restoring Vision to the Blind with Chemical Photoswitches. *Chem Rev* **2018,** *118* (21), 10748-10773.

23.   Beharry, A. A.; Sadovski, O.; Woolley, G. A., Azobenzene photoswitching without ultraviolet light. *J Am Chem Soc* **2011,** *133* (49), 19684-7.

24.   Martinez-Lopez, D.; Babalhavaeji, A.; Sampedro, D.; Woolley, G. A., Synthesis and characterization of bis(4-amino-2-bromo-6-methoxy)azobenzene derivatives. *Beilstein J Org Chem* **2019,** *15*, 3000-3008.

25.   Garcia-Amoros, J.; Velasco, D., Recent advances towards azobenzene-based light-driven real-time information-transmitting materials. *Beilstein J Org Chem* **2012,** *8*, 1003-17.

26.   Lameijer, L. N.; Budzak, S.; Simeth, N. A.; Hansen, M. J.; Feringa, B. L.; Jacquemin, D.; Szymanski, W., General Principles for the Design of Visible-Light-Responsive Photoswitches: Tetra-ortho-Chloro-Azobenzenes. *Angew Chem Int Ed Engl* **2020,** *59* (48), 21663-21670.

27.   Hansen, M. J.; Lerch, M. M.; Szymanski, W.; Feringa, B. L., Direct and Versatile Synthesis of Red-Shifted Azobenzenes. *Angew Chem Int Ed Engl* **2016,** *55* (43), 13514-13518.

28.   Lerch, M. M.; Hansen, M. J.; van Dam, G. M.; Szymanski, W.; Feringa, B. L., Emerging Targets in Photopharmacology. *Angew Chem Int Ed Engl* **2016,** *55* (37), 10978-99.

29.   Szymanski, W.; Beierle, J. M.; Kistemaker, H. A.; Velema, W. A.; Feringa, B. L., Reversible photocontrol of biological systems by the incorporation of molecular photoswitches. *Chem Rev* **2013,** *113* (8), 6114-78.

30.   Beharry, A. A.; Sadovski, O.; Woolley, G. A., Azobenzene Photoswitching without Ultraviolet Light. *Journal of the American Chemical Society* **2011,** *133* (49), 19684-19687.

31.   Samanta, S.; Babalhavaeji, A.; Dong, M. X.; Woolley, G. A., Photoswitching of ortho-substituted azonium ions by red light in whole blood. *Angew Chem Int Ed Engl* **2013,** *52* (52), 14127-30.

32.   Dong, M.; Babalhavaeji, A.; Collins, C. V.; Jarrah, K.; Sadovski, O.; Dai, Q.; Woolley, G. A., Near-Infrared Photoswitching of Azobenzenes under Physiological Conditions. *J Am Chem Soc* **2017,** *139* (38), 13483-13486.

33.   Coelho, P. J.; Carvalho, L. M.; Fonseca, A. M. C.; Raposo, M. M. M., Photochromic properties of thienylpyrrole azo dyes in solution. *Tetrahedron Letters* **2006,** *47* (22), 3711-3714.

34.   Simke, J.; Bosking, T.; Ravoo, B. J., Photoswitching of ortho-Aminated Arylazopyrazoles with Red Light. *Org Lett* **2021,** *23* (19), 7635-7639.

35.   Wang, Y. T.; Liu, X. Y.; Cui, G.; Fang, W. H.; Thiel, W., Photoisomerization of Arylazopyrazole Photoswitches: Stereospecific Excited-State Relaxation. *Angew Chem Int Ed Engl* **2016,** *55* (45), 14009-14013.

36.   Weston, C. E.; Richardson, R. D.; Fuchter, M. J., Photoswitchable basicity through the use of azoheteroarenes. *Chem Commun (Camb)* **2016,** *52* (24), 4521-4.

37.   Wendler, T.; Schutt, C.; Nather, C.; Herges, R., Photoswitchable azoheterocycles via coupling of lithiated imidazoles with benzenediazonium salts. *J Org Chem* **2012,** *77* (7), 3284-7.

38.   Otsuki, J.; Suwa, K.; Narutaki, K.; Sinha, C.; Yoshikawa, I.; Araki, K., Photochromism of 2-(Phenylazo)imidazoles, *J. Phys. Chem. A.,* **2005,** *109,* 8064-8069.

39.   Otsuki, J,; Suwa, K.; Sarker, K. K.; Sinha, C., Photoisomerization and Thermal Isomerization of Arylazoimidazoles, *J. Phys. Chem. A.,* **2007,** *111,* 1403-1409.

40.   Qian, H.; Wang, Y. Y.; Guo, D. S.; Aprahamian, I., Controlling the Isomerization Rate of an Azo-BF2 Switch Using Aggregation. *J Am Chem Soc* **2017,** *139* (3), 1037-1040.

41.   Yang, Y.; Hughes, R. P.; Aprahamian, I., Visible light switching of a BF2-coordinated azo compound. *J Am Chem Soc* **2012,** *134* (37), 15221-4.

42.   Konrad, D. B.; Savasci, G.; Allmendinger, L.; Trauner, D.; Ochsenfeld, C.; Ali, A. M., Computational Design and Synthesis of a Deeply Red-Shifted and Bistable Azobenzene. *J Am Chem Soc* **2020,** *142* (14), 6538-6547.

43.   Konrad, D. B.; Frank, J. A.; Trauner, D., Synthesis of Redshifted Azobenzene Photoswitches by Late-Stage Functionalization. *Chemistry – A European Journal* **2016,** *22* (13), 4364-4368.

44.   Heindl, A. H.; Wegner, H. A., Rational Design of Azothiophenes-Substitution Effects on the Switching Properties. *Chemistry* **2020,** *26* (60), 13730-13737.

45.   Slavov, C.; Yang, C.; Heindl, A. H.; Wegner, H. A.; Dreuw, A.; Wachtveitl, J., Thiophenylazobenzene: An Alternative Photoisomerization Controlled by Lone-Pairpi Interaction. *Angew Chem Int Ed Engl* **2020,** *59* (1), 380-387.

46.   He, Y.; Shangguan, Z.; Zhang, Z. Y.; Xie, M.; Yu, C.; Li, T., Azobispyrazole Family as Photoswitches Combining (Near-) Quantitative Bidirectional Isomerization and Widely Tunable Thermal Half-Lives from Hours to Years*. *Angew Chem Int Ed Engl* **2021,** *60* (30), 16539-16546.

47.   Calbo, J.; Weston, C. E.; White, A. J.; Rzepa, H. S.; Contreras-Garcia, J.; Fuchter, M. J., Tuning Azoheteroarene Photoswitch Performance through Heteroaryl Design. *J Am Chem Soc* **2017,** *139* (3), 1261-1274.

48.   Calbo, J.; Thawani, A. R.; Gibson, R. S. L.; White, A. J. P.; Fuchter, M. J., A combinatorial approach to improving the performance of azoarene photoswitches. *Beilstein J Org Chem* **2019,** *15*, 2753-2764.

49.   Weston, C. E.; Richardson, R. D.; Haycock, P. R.; White, A. J.; Fuchter, M. J., Arylazopyrazoles: azoheteroarene photoswitches offering quantitative isomerization and long thermal half-lives. *J Am Chem Soc* **2014,** *136* (34), 11878-81.

50.   Broichhagen, J.; Frank, J. A.; Johnston, N. R.; Mitchell, R. K.; Smid, K.; Marchetti, P.; Bugliani, M.; Rutter, G. A.; Trauner, D.; Hodson, D. J., A red-shifted photochromic sulfonylurea for the remote control of pancreatic beta cell function. *Chem Commun (Camb)* **2015,** *51* (27), 6018-21.

51.   Crespi, S.; Simeth, N. A.; König, B., Heteroaryl azo dyes as molecular photoswitches. *Nature Reviews Chemistry* **2019,** *3* (3), 133-146.

52.   Coelho, P. J.; Sousa, C. M.; Castro, M. C. R.; Fonseca, A. M. C.; Raposo, M. M. M., Fast thermal cis–trans isomerization of heterocyclic azo dyes in PMMA polymers. *Optical Materials* **2013,** *35* (6), 1167-1172.

53.   Wannipurage, D.; Kurup, S. S.; Groysman, S., Heterocoupling of Different Aryl Nitrenes to Produce Asymmetric Azoarenes Using Iron–Alkoxide Catalysis and Investigation of the Cis–Trans Isomerism of Selected Bulky Asymmetric Azoarenes. *Organometallics* **2021,** *40* (21), 3637-3644.

54.   Xu, Y.; Gao, C.; Andréasson, J.; Grøtli, M., Synthesis and Photophysical Characterization of Azoheteroarenes. *Organic Letters* **2018,** *20* (16), 4875-4879.

55.   Yin, T.-T.; Zhao, Z.-X.; Zhang, H.-X., A theoretical study on the thermal cis–trans isomerization of azoheteroarene photoswitches. *New Journal of Chemistry* **2017,** *41* (4), 1659-1669.

56.   Crecca, C. R.; Roitberg, A. E., Theoretical study of the isomerization mechanism of azobenzene and disubstituted azobenzene derivatives. *J Phys Chem A* **2006,** *110* (26), 8188-203.

57.   Gagliardi, L.; Orlandi, G.; Bernardi, F.; Cembran, A.; Garavelli, M., A theoretical study of the lowest electronic states of azobenzene: the role of torsion coordinate in the cis–trans photoisomerization. *Theoretical Chemistry Accounts* **2003,** *111* (2-6), 363-372.

58.   Muzdalo, A.; Saalfrank, P.; Vreede, J.; Santer, M., Cis-to- Trans Isomerization of Azobenzene Derivatives Studied with Transition Path Sampling and Quantum Mechanical/Molecular Mechanical Molecular Dynamics. *J Chem Theory Comput* **2018,** *14* (4), 2042-2051.

59.   Dokic, J.; Gothe, M.; Wirth, J.; Peters, M. V.; Schwarz, J.; Hecht, S.; Saalfrank, P., Quantum chemical investigation of thermal cis-to-trans isomerization of azobenzene derivatives:

substituent effects, solvent effects, and comparison to experimental data. *J Phys Chem A* **2009,** *113* (24), 6763-73.

60.   Robertus, J.; Reker, S. F.; Pijper, T. C.; Deuzeman, A.; Browne, W. R.; Feringa, B. L., Kinetic analysis of the thermal isomerisation pathways in an asymmetric double azobenzene switch. *Phys Chem Chem Phys* **2012,** *14* (13), 4374-82.

61.   Asano, T.; Okada, T.; Shinkai, S.; Shigematsu, K.; Kusano, Y.; Manabe, O., Temperature and pressure dependences of thermal cis-to-trans isomerization of azobenzenes which evidence an inversion mechanism. *Journal of the American Chemical Society* **2002,** *103* (17), 5161-5165.

62.   Huddleston, P. R.; Volkov, V. V.; Perry, C. C., The structural and electronic properties of 3,3'-azothiophene photo-switching systems. *Phys Chem Chem Phys* **2019,** *21* (3), 1344-1353.

63.   Devi, S.; Saraswat, M.; Grewal, S.; Venkataramani, S., Evaluation of Substituent Effect in Z-Isomer Stability of Arylazo-1 H-3,5-dimethylpyrazoles: Interplay of Steric, Electronic Effects and Hydrogen Bonding. *J Org Chem* **2018,** *83* (8), 4307-4322.

64.   Stricker, L.; Bockmann, M.; Kirse, T. M.; Doltsinis, N. L.; Ravoo, B. J., Arylazopyrazole Photoswitches in Aqueous Solution: Substituent Effects, Photophysical Properties, and Host-Guest Chemistry. *Chemistry* **2018,** *24* (34), 8639-8647.

65.   Zhang, Z. Y.; He, Y.; Zhou, Y.; Yu, C.; Han, L.; Li, T., Pyrazolylazophenyl Ether-Based Photoswitches: Facile Synthesis, (Near-)Quantitative Photoconversion, Long Thermal Half-Life, Easy Functionalization, and Versatile Applications in Light-Responsive Systems. *Chemistry* **2019,** *25* (58), 13402-13410.

66.   Abreha, B. G.; Agarwal, S.; Foster, I.; Blaiszik, B.; Lopez, S. A., Virtual Excited State Reference for the Discovery of Electronic Materials Database: An Open-Access Resource for Ground and Excited State Properties of Organic Molecules. *J Phys Chem Lett* **2019,** *10* (21), 6835-6841.

67.   Batsyts, S.; Hübner, E. G.; Namyslo, J. C.; Schmidt, A., The Interconnection of Two Positive Charges by Conjugation and Cross-Conjugation in Bis-Quinolinium Ethynyls. *European Journal of Organic Chemistry* **2019,** *2019* (36), 6168-6176.

68.   Ting, J. Y. C.; Roseli, R. B.; Krenske, E. H., How does cross-conjugation influence thiol additions to enones? A computational study of thiol trapping by the naturally occurring divinyl ketones zerumbone and alpha-santonin. *Org Biomol Chem* **2020,** *18* (7), 1426-1435.

69.   Halskov, K. S.; Johansen, T. K.; Davis, R. L.; Steurer, M.; Jensen, F.; Jorgensen, K. A., Cross-trienamines in asymmetric organocatalysis. *J Am Chem Soc* **2012,** *134* (31), 12943-6.

70.   Dieckmann, A.; Breugst, M.; Houk, K. N., Zwitterions and unobserved intermediates in organocatalytic Diels-Alder reactions of linear and cross-conjugated trienamines. *J Am Chem Soc* **2013,** *135* (8), 3237-42.

71.   Ishiuchi, K. i.; Kubota, T.; Hayashi, S.; Shibata, T.; Kobayashi, J. i., Lycopladine H, a novel alkaloid with fused-tetracyclic skeleton from Lycopodium complanatum. *Tetrahedron Letters* **2009,** *50* (47), 6534-6536.

72.   Li, D.; Wang, F.; Cai, S.; Zeng, X.; Xiao, X; Gu, Q,; Zhu, W., Two New Bisorbicillinoids Isolated from a Deep-sea Fungus *Phialocephala* sp. FL30r, *J. Antibiot.* **2007,** *60*(5), 317-320.

73.   Huang, J.; Yokoyama, R.; Yang, C.; Fukuyama, Y., Structure and Neurotrophic Activity of *seco*-Prezisaane-Type Sesquiterpenes from *Illicium merrillianum, J. Nat. Prod,* **2001,** *64*¸428-431.

74.   Schomaker, V.; Pauling, L., The Electron Diffraction Investigation of the Structure of Benzene, Pyridine, Pyrazine, Butadiene-1,3, Cyclopentadiene, Furan, Pyrrole, and Thiophene. *Journal of the American Chemical Society* **2002,** *61* (7), 1769-1780.

75.   Adrion, D. M.; Kaliakin, D. S.; Neal, P.; Lopez, S. A., Benchmarking of Density Functionals for Z-Azoarene Half-Lives via Automated Transition State Search. *J Phys Chem A* **2021**.

76.   Frisch, M. J.; Trucks, G. W.; Schlegel, H. B.; Scuseria, G. E.; Robb, M. A.; Cheeseman, J. R.; Scalmani, G.; Barone, V.; Petersson, G. A.; Nakatsuji, H.; Li, X.; Caricato, M.; Marenich, A. V.; Bloino, J.; Janesko, B. G.; Gomperts, R.; Mennucci, B.; Hratchian, H. P.; Ortiz, J. V.; Izmaylov, A. F.; Sonnenberg, J. L.; Williams; Ding, F.; Lipparini, F.; Egidi, F.; Goings, J.; Peng, B.; Petrone, A.; Henderson, T.; Ranasinghe, D.; Zakrzewski, V. G.; Gao, J.; Rega, N.; Zheng, G.; Liang, W.; Hada, M.; Ehara, M.; Toyota, K.; Fukuda, R.; Hasegawa, J.; Ishida, M.; Nakajima, T.; Honda, Y.; Kitao, O.; Nakai, H.; Vreven, T.; Throssell, K.; Montgomery Jr., J. A.; Peralta, J. E.; Ogliaro, F.; Bearpark, M. J.; Heyd, J. J.; Brothers, E. N.; Kudin, K. N.; Staroverov, V. N.; Keith, T. A.; Kobayashi, R.; Normand, J.; Raghavachari, K.; Rendell, A. P.; Burant, J. C.; Iyengar, S. S.; Tomasi, J.; Cossi, M.; Millam, J. M.; Klene, M.; Adamo, C.; Cammi, R.; Ochterski, J. W.; Martin, R. L.; Morokuma, K.; Farkas, O.; Foresman, J. B.; Fox, D. J. *Gaussian 16 Rev. C.01*, Wallingford, CT, 2016.
77.   Adamo, C.; Barone, V., Toward reliable density functional methods without adjustable parameters: The PBE0 model. *The Journal of Chemical Physics* **1999,** *110* (13), 6158-6170.
78.   Ditchfield, R.; Hehre, W. J.; Pople, J. A., Self-Consistent Molecular-Orbital Methods. IX. An Extended Gaussian-Type Basis for Molecular-Orbital Studies of Organic Molecules. *The Journal of Chemical Physics* **1971,** *54* (2), 724-728.
79.   Furche, F.; Ahlrichs, R., Adiabatic time-dependent density functional methods for excited state properties. *The Journal of Chemical Physics* **2002,** *117* (16), 7433-7447.
80.   Chai, J. D.; Head-Gordon, M., Long-range corrected hybrid density functionals with damped atom-atom dispersion corrections. *Phys Chem Chem Phys* **2008,** *10* (44), 6615-20.
81.   Tomasi, J.; Mennucci, B.; Cammi, R., Quantum mechanical continuum solvation models. *Chem Rev* **2005,** *105* (8), 2999-3093.